A Transcriptome-Based Molecular Taxonomy for Non-Surgical Thyroid Eye Disease: A Cross-Sectional Cohort Study with Unsupervised Clustering

Tianyi Zhu[1,2,3,4,†], Weijin Qian[1,2,3,4,†], Jin Liu[1,2,3,4,†], Qiang Huang[5], Lianfei Fang[1,2,3,4], Li Yang[1,2,3,4], Runchuan Li[1,2,3,4], Xuefei Song[1,2,3,4], Liang Chen[5], Huifang Zhou[1,2,3,4,*]

[1]Department of Ophthalmology, Shanghai Ninth People's Hospital, Shanghai Jiao Tong University School of Medicine, Shanghai, China

[2]Shanghai Key Laboratory of Orbital Diseases and Ocular Oncology, Shanghai, China

[3]Center for Basic Medical Research and Innovation in Visual System Diseases of Ministry of Education, Shanghai, China

[4]Chinese Consortium for Thyroid Eye Disease (CCTED), Shanghai, China

[5]State Key Laboratory of New Targets Discovery and Drug Development for Major Diseases, School of Medicine, Shanghai University, Shanghai, China

[†]These authors contributed equally to this work and share first authorship.

**Corresponding Author*

Abstract: An autoimmune condition affecting the orbit, known as thyroid eye disease (TED), commonly presents in conjunction with Graves' hyperthyroidism (GH). Current severity and activity assessments do not effectively inform treatment regimens, particularly the selection of target therapies for non-surgical TED. Our research aimed to develop a new TED classifier to improve the diagnosis and to aid in the precise treatment. A three-arm cohort of 224 participants including patients with TED and GH, as well as healthy controls was collected at baseline before treatment for RNA sequencing. Differential analysis revealed gene expression signatures that were unique to TED. Unsupervised clustering based on ophthalmopathy-specific genes and most variable genes was conducted in TED. This classification was validated by bootstrap resampling and refined using biological hub genes for clinical applications. Clinical manifestations, immune infiltration, and drug sensitivity were analysed in different TED subtypes. In TED, autoantigens were elevated, immune responses were activated, and both cellular proliferation and metabolic disorders were observed. A new molecular taxonomy was established and validated that is complementary to the severity and activity in guidelines. C1 (n=93) was the "adaptive and proliferative" subtype, characterised by an increased number of adaptive lymphocytes and represented by six hub genes (DDR2, LRP1B, NTRK2, PALB2, PTPRD and SLC25A6). In contrast, C2 (n=59) was the "inflammatory and destructive" subtype, exhibiting greater pain and reflex epiphora symptom, and represented by three hub genes (MON2, SNORA74B and STX16). There were significant differences in clinical characteristics, risk factors, ocular pain and reflex epiphora. Drug sensitivity analysis revealed distinct therapeutic vulnerabilities for the two subtypes: C1 showed sensitivity to kinase inhibitors, while C2 showed sensitivity to glucocorticoids and anti-inflammatory agents. We profiled the genes of TED and developed a hub gene-based molecular classification, which provides a framework for subtype-guided therapeutic selection.

Keywords: Thyroid Eye Disease; Molecular Taxonomy; Unsupervised Clustering; Transcriptome Sequencing; Targeted Therapy.

1. Introduction

Thyroid eye disease (TED) shows a strong association with Graves' disease. While the majority of cases occur in patients with hyperthyroidism, a subset of patients present with euthyroid or hypothyroid status[1]. Approximately 40% of patients with Graves' disease suffer from TED symptoms, and the rate rises to 70% when taking imaging examinations

are taken into consideration[2]. TED pathogenesis begins with the activation of two autoantigens located on orbital fibroblasts, the thyroid stimulating hormone receptor (TSHR) and the insulin-like growth factor 1 receptor (IGF-1R)[3]. The estimated prevalence of TED is 90~305/100,000 per year, causing a significant public health concern worldwide[4]. Beyond its heterogeneous clinical manifestations, TED also imposes a heavy psychosocial burden[5]. Therefore, it is crucial to delineate the distinct pathology of TED and optimize its diagnostic and therapeutic strategies.

According to the established guidelines, the formulation of treatment for TED is guided by activity and severity. However, it should be noted that the efficacy of this approach is constrained by various limitations[6]. Patients with active moderate-to-severe TED worth the largest proportion, and intravenous corticosteroids are the primary treatment for this group. However, the response rate of intravenous corticosteroids is only 65~70%[7], while the post-treatment recurrence rate can be as high as 20~40%[8]. There is growing enthusiasm for new targeted agents that interfere with autoimmune mechanisms, many of which have advanced to clinical use or investigation. It has been reported that teprotumumab is effective in both activity phases. Furthermore, it has been demonstrated to be effective in cases of dysthyroid optic neuropathy[9-11]. However, subsequent long-term observation demonstrated a decline in its effectiveness, with response rates for proptosis and diplopia not exceeding 70%[12]. Collectively, a key challenge is the unclear criteria for identifying the ideal patient subgroups for these agents, leading to subjective treatment decisions and unnecessary costs.

Consequently, further subtyping of TED post-diagnosis is imperative for precision medicine, as evidenced by preliminary studies exploring this approach. In light of the insidious onset and varied prognoses characteristic of eye symptoms, our previous research proposed the use of early diagnostic biomarkers of TED based on characteristic gene expression signatures[13,14]. The present study proposes a further stratification of non-surgical patients into subgroups following a TED diagnosis, with a view to facilitating the selection of appropriate therapies. Additionally, an imaging-based classification for TED has been proposed: Typically, the classification hinges on whether adipose tissue or extraocular muscle volume predominates within the total orbital volume[15,16]. Other dimensions to classify TED include duration, autoantibody types, cytokine expression profiles[17-19]. Nevertheless, the challenge of selecting appropriate medications for non-surgical patients, who account for the largest proportion of TED patients, remains unresolved. Consequently, there is an urgent requirement for improvements in the molecular classification of TED to enhance diagnostic accuracy and guide treatment. In this study, we sought to identify distinct gene expression signatures and specific gene sets associated with ophthalmopathy in patients diagnosed with TED. To this end, we undertook a comparative examination of the peripheral blood transcriptomes from TED, GH and healthy controls (HC). A molecular classification for TED was established on the basis of the overlap gene set of highly variable genes and ophthalmopathy-specific genes. It was then validated due to its high robustness. Two subtypes of non-surgical TED were defined and displayed significantly different clinical manifestations, immune infiltration, and drug sensitivity. The application of the classification is expected to be accelerated by refined hub genes. This approach will complement the existing activity and severity to form a three-dimensional evaluation system to guide TED pharmacotherapy.

2. Methods

2.1 Participants

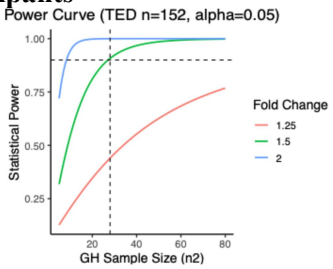

Figure 1. Power Analysis for Sample Size Determination in the GH Group

Table 1. Inclusion Criteria for Both TED and GH Patients

Item	Inclusion criteria
Age	From 18 to 75 years old
Sex	No gender preference
Race	Han population
Duration	At least 6 months since hyperthyroidism was diagnosed
Treatment	No intravenous or oral glucocorticoids,

history	immunosuppressants, targeted drugs, orbital surgery, radiation therapy, or radioactive iodine therapy within 6 months; using only medications for hyperthyroidism when sampling
Other diseases	No other systemic diseases such as hypertension, diabetes mellitus, tumors, other autoimmune diseases, cardiac/hepatic/renal insufficiency and any existing acute or chronic infections
COVID-19	At least 3 months since last infection, at least 3 months since last vaccination
Pregnancy history	Not during pregnancy and breastfeeding

Table 2. Inclusion and Exclusion Criteria for Health Controls

Item	Criteria
Inclusion	
Age	From 18 to 75 years old
Sex	No gender preference
Race	Han population
COVID-19	At least 3 months since last infection, at least 3 months since last vaccination
Pregnancy history	Not during pregnancy and breastfeeding
Graves' disease	Normal thyroid function tests (TSH, fT3, fT4, TRAb) and the absence of any ocular symptoms
Exclusion	
Iodine drugs	Use of iodine-containing medications or iodinated contrast media within the past 3 months
Radioiodine	History of exposure to radioiodine therapy
Systemic drugs	Use of glucocorticoids, immunosuppressants, or targeted therapeutic agents within the past year
Vaccination	Administration of any vaccine within the past 6 months
Other Diseases	Presence of any autoimmune disease, malignancy, acute infection, chronic systemic metabolic disease, or cardiopulmonary insufficiency

Table 3. Clinical Data Collected from TED Patients

Category	Item
Demographic information	Sex, age, smoking habit, years of education
Thyroid disease conditions	Disease duration, treatment history, latest thyroid function report, latest liver and kidney function report
Eye disease conditions	Activity, severity, symptoms, signs, orbital CT or MRI, disease duration, treatment history
Ocular examination results	Visual acuity, intraocular pressure, exophthalmos, degree of strabismus, diplopia score, MRD, CAS, Schirmer, BUT
Psycho-psychological scales	Visual function score[a], social conversion score[b], anxiety score[c], depression score[d]

[a, b]GO-QOL questionnaire (Terwee, 1998)
[c]HARS (Hamilton, 1960)
[d]HDRS (Hamilton, 1967)

A total of 152 patients with TED, 20 patients diagnosed with GH, and 52 HC were retrieved from Shanghai Ninth People's Hospital over the period from 2022 to 2024. The sequencing data are available in the Gene Expression Omnibus (GSE280114[20] and GSE285190[21]). Because GH patients meeting the inclusion criteria were scarce, a retrospective power analysis was completed by using the R package "RNASeqPower" to ensure that the GH sample size was statistically sound (Figure 1). In accordance with the Declaration of Helsinki, this study was approved by the ethics committee and institutional review board of Shanghai Ninth People's Hospital (SH9H-2025-T502-1). The subjects were recruited in align with the inclusion and exclusion criteria (Table 1- Table 2). Their clinical information (Table 3) and peripheral blood mononuclear cells (PBMC) for RNA sequencing were collected (Figure 2). The clinical assessments of disease activity and severity were performed in accordance with the criteria defined in the 2022 joint expert consensus[6].

With the TED group size fixed at 152, a minimum of 19 samples in the GH group is required to achieve 90% power (1.5-fold change, α=0.05, CV=0.4, mean count=10).

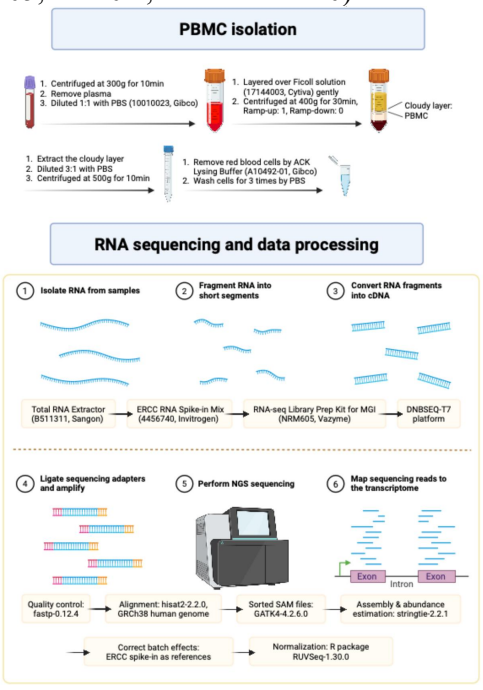

Figure 2. Protocol for PBMC Isolation and RNA Sequencing
(This figure was created with BioRender.com and is used with permission.)

2.2 PBMC Isolation

Collected peripheral blood samples were put in EDTA anticoagulant tubes, constantly kept at 4°C, and immediately processed. PBMC isolation was performed using a Ficoll density gradient centrifugation procedure. Diluted 1:1 with phosphate buffered saline, whole blood samples were softly added onto Ficoll. The mixture was then subjected to a centrifugal process at 400g for a duration of 30 minutes at ambient temperature. The acceleration and brake settings of the centrifuge apparatus were configured to 1. Following centrifugation, the intermediate layer of PBMC was collected with the utmost care. This layer was then subjected to a centrifugation process at 500g for a duration of 10 minutes at ambient temperature. The resulting PBMC pellet was subjected to a further wash with phosphate buffered saline and subsequently subjected to centrifugation in order to enrich the cells. Samples with substantial red blood cell contamination were treated with ACK Lysing Buffer (A10492-01, Gibco) for red blood cell lysis.

2.3 RNA Sequencing and Data Processing

Total RNA Extractor (B511311, Sangon) was used to get the pure RNA. The total RNA was then mixed with ERCC RNA Spike-in Mix (4456740, Invitrogen) in proportion for the construction of the transcriptome library. The preparation of the sequencing library was undertaken using the RNA-seq Library Prep Kit for MGI (NRM605, Vazyme), and the library was subsequently tested in batches on DNBSEQ-T7. The fastq data were submitted to quality control through fastp-0.12.4. Alignment was performed using hisat2-2.2.0, with the GRCh38 human genome serving as the reference, which included ERCC spike sequences. Sorted SAM files were processed using GATK4-4.2.6.0, and transcript assembly and abundance estimation were carried out using stringtie-2.2.1. Batch effects were corrected using ERCC spike-in as references, employing the R package RUVSeq-1.30.0 for normalization.

2.4 Differential Analysis, Unsupervised Clustering with Validation

Differential expression analysis was conducted by the “DESeq2” R package. Genes were considered differentially expressed if they met the following criteria: $|\log2\ FC| > \log2(1.5)$ and p-value < 0.05[22]. The functional enrichment pathways were detected by the R package "clusterProfiler" with the Gene Ontology (GO)[23] and Kyoto Encyclopedia of Genes and Genomes (KEGG)[24] databases were used to perform functional enrichment analysis by "clusterProfiler" R package[25]. Gene set enrichment analysis (GSEA) with REACTOME and GO subsets from molecular signatures database (MsigDB) were implemented (normalized enrichment score > 0)[26,27]. The "ConsensusClusterPlus" R package was utilised for the purpose of achieving consistent clustering[28]. The robustness of the consensus clustering result was validated using bootstrap resampling by adjusted rand index (ARI).

2.5 Analyses on Immune Infiltration, Hub Genes and Drug Sensitivity

Single-sample GSEA (ssGSEA), a method based on gene sets of 28 immune cell subtypes, was used to analyze immune infiltration[29,30]. Weighted gene co-expression network analysis (WGCNA) identified unique gene modules for the two clusters[31]. Preliminary hub genes were screened as with module membership (MM) > 0.8 and gene significance (GS) > 0.2, followed by LASSO regression analysis of candidate genes from the greenyellow and green modules to identify the key hub genes. Potential sensitive drugs with different mechanisms were screened using the Connectivity Map (CMap) database. The visualisation of these modules was achieved by "OncoPrint" in R[32,33].

2.6 Statistical Analysis

Transcriptomic analyses were did by R (Version 4.4.0). The T-test was chosen for comparing continuous variables. For categorical variables, the Chi-Square or Fisher's exact test was utilised. Finally, the Pearson correlation test was implemented to investigate the GS-MM correlation. The statistical software SPSS 29.0.1.0 (SPSS Inc., Chicago, IL, USA) was utilised for the purpose of comparing clinical manifestations. All tests were two-sided, and a p-value of less than 0.05 was considered statistically significant.

2.7 Schematics

Graphs was facilitated by Adobelllustrator (v 25.4.1) and BioRender.com.

3. Results

3.1 TED Exhibited Enhanced Autoimmune Responses, Cell Proliferation and Energy Metabolism

A large-scale cohort was established (Figure 3) comprising 152 patients with TED, 20 patients with GH without eye disease and 52 healthy controls. As demonstrated in Table 4, a balanced distribution of sex and age was observed between the TED and HC groups, as well as between the TED and GH groups. Analyzing differential gene expression, we identified a distinct transcriptomic profile in TED patients compared to HC, with 250 genes significantly overexpressed and 165 genes underexpressed. It is noteworthy that several genes associated with tissue remodelling and oncogenesis, including ALK receptor tyrosine kinase (ALK), BRCA1 DNA repair associated (BRCA1), and RET proto-oncogene (RET), were among the most significantly altered features in the volcano plot (Figure 4A). These DEGs were predominantly involved in immune response regulation, inflammatory cell activation, and metabolic processes, as revealed by subsequent GO enrichment analysis. This further supports the systemic nature of TED pathogenesis (Figure 4B). Similar to GO findings, KEGG further identified significant enrichment of several immune- and metabolism-related processes, including chemokine pathways, cytokine-cytokine receptor activation, and oxidative phosphorylation, suggesting crosstalk between inflammation and metabolic reprogramming in TED (Figure 4C).

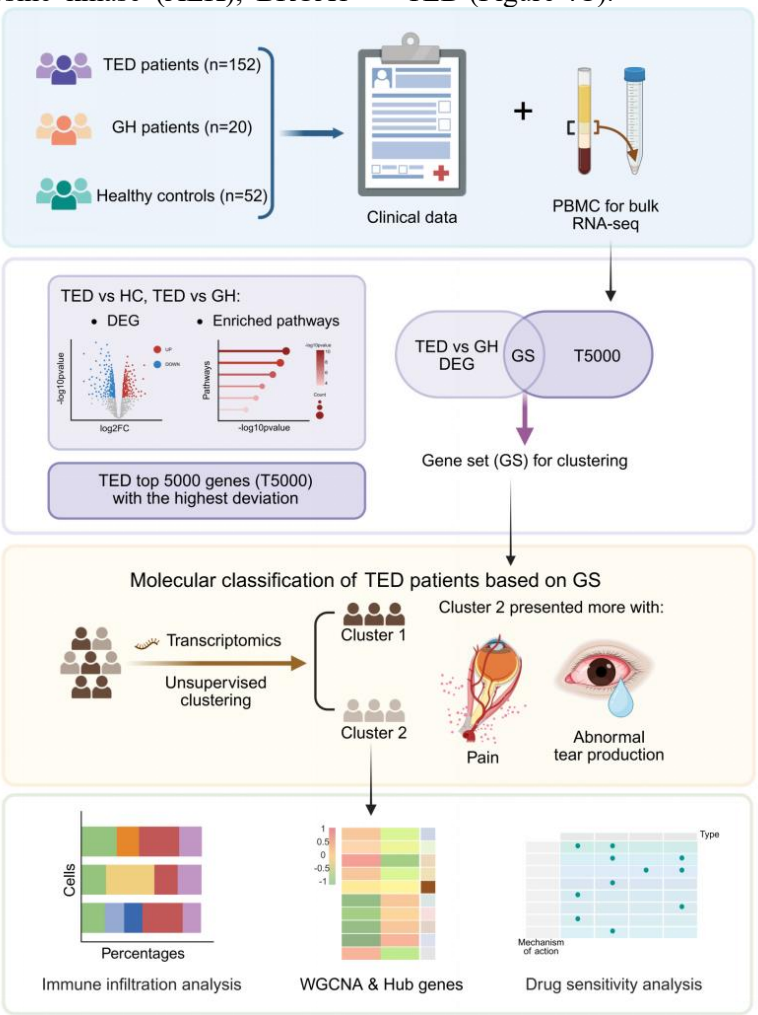

Figure 3. Schematic Graphic of the Study

A cohort of TED comprising 152 patients, 20 GH patients without eye disease and 52 HC was established with standardized clinical data with PBMC collected. Unsupervised clustering on the intersecting gene set of DEGs and high genes among TED divided TED patients into two subtypes. Clinical phenotyping, immune infiltration analysis, hub genes identification, and drug sensitivity prediction were conducted for the new two subtypes.

(This figure was created with BioRender.com and is used with permission.)

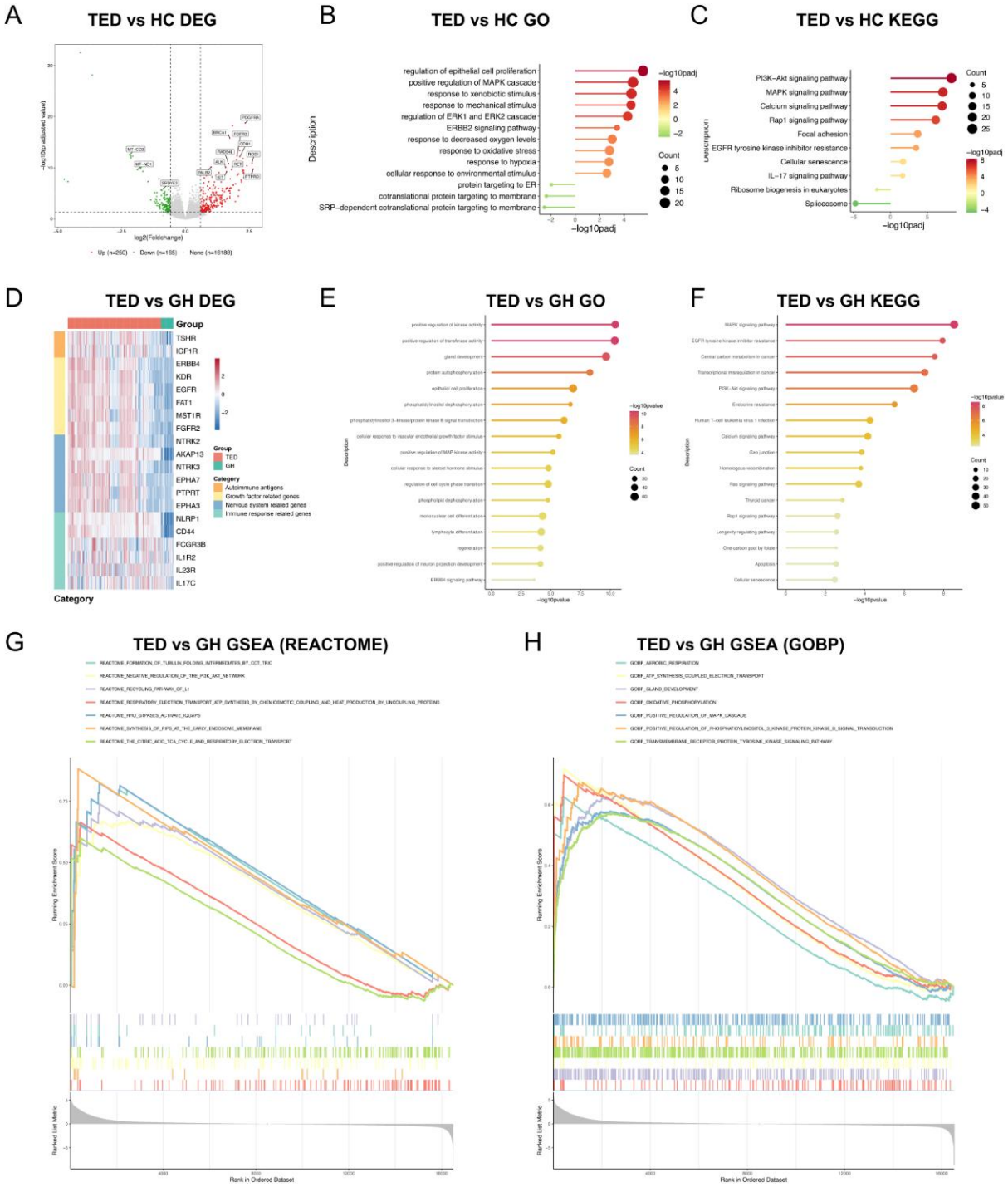

Figure 4. Different Gene Profile (TED vs HC/GH)

(A) Volcano plot illustrated DEGs (TED vs HC) with 250 upregulated genes and 165 downregulated genes. **(B)** GO analysis based on DEGs (TED vs HC). **(C)** KEGG analysis based on DEGs (TED vs HC). **(D)** Core Transcriptomic Signatures (TED vs GH). **(E)** GO analysis based on upregulated genes (TED vs GH). **(F)** KEGG analysis based on upregulated genes (TED vs GH). **(G)** GSEA showed upregulated pathways (TED vs GH) based on REACTOME database. **(H)** GSEA pictured upregulated pathways (TED vs GH) based on GOBP database.

In the subsequent stage of the study, a comparison was made between patients suffering from TED and those suffering from GH, with a view to controlling for the effects of hyperthyroidism and identifying transcriptomic features specific to ophthalmopathy. Principal component analysis (PCA) showed that TED and GH gene profiles differed observably (Figure 5A). 2088 DEGs were upregulated, while 925 DEGs were downregulated in TED

(Figure 5B-C). The genes that were found to be significantly more active can be divided into three groups: (1) receptor tyrosine kinases and phosphatases: Erb-B2 receptor tyrosine kinase 4 (ERBB4), epidermal growth factor receptor (EGFR), fibroblast growth factor receptor 2 (FGFR2), neurotrophic receptor tyrosine kinase 2/3 (NTRK2/3), and protein tyrosine phosphatase receptor type T (PTPRT); (2) cytokines and their receptors: interleukin 1 receptor type 2 (IL1R2), interleukin 23 receptor (IL23R) and interleukin 17C (IL17C); (3) immune cell surface molecules: CD44 and Fc gamma receptor IIIb (FCGR3B); and autoantigens (Figure 4D). It is noteworthy that TSHR and IGF-1R levels were markedly increased in TED (log2 FC = 1.70, p-value < 0.001; log2 FC = 0.304, p-value = 0.001) (Figure 4D).

GO analysis showed that the pathways significantly enriched in biological processes in TED included growth factor activity, signal transduction, cell proliferation, immune cell differentiation, tissue remodelling and neuronal projection development (Figure 4E). KEGG Analysis yielded results consistent with the aforementioned findings, revealing upregulation of pathways involved in cell proliferation, energy metabolism, immune activation, and immunosenescence in TED (Figure 4F). GSEA revealed that oxidative phosphorylation, respiratory electron transport and adenosine triphosphate synthesis coupled electron transport were elevated in TED, suggesting more vigorous energy metabolism (Figure 4G-H).

Collectively, DEGs and functional enrichment analysis collectively confirmed that TED was associated with hyperactive immune responses, augmented cellular proliferation, and metabolic reprogramming.

Table 4. Basic Information of the Participants Included

	TED	GH	HC	p-value
No. of participants included	152	20	52	
Sex, M/F	52/100	7/13	21/31	0.944 (vs GH) 0.423 (vs HC)
Age, mean±SD (range), y	42.88±13.25 (18-74)	39.70±13.05 (23-63)	42.69±14.20 (20-65)	0.347 (vs GH) 0.897 (vs HC)
Duration of TED, median (IQR), m	13 (6-30)	NA	NA	NA
Duration of hyperthyroidism, median (IQR), m	21.5 (10-44)	8 (7-12)	NA	0.002 (vs GH)

The statistical significance of age was assessed through the implementation of a two-sided t-test, given the near-normal distribution of the data and the presence of a chi-squared variance between the two groups. The assessment of statistical significance for the duration of TED and hyperthyroidism was conducted using a two-sided rank sum test, because they were not normal distributed. The statistical significance of sex was determined through the utilisation of a chi-square test.

3.2 Transcriptome Profiling of TED Revealed Two Molecular Subtypes

The intersection of the DEGs and TED hypervariable gene set (comprising the top 5000 variable genes among TED patients) was utilised to derive a novel gene set consisting of 1611 genes. The study revealed that the sample reflected eye disease-specific features and exhibited the most significant variation among TED patients (Figure 6A). Unsupervised clustering was performed using the new gene set, and the optimal count of clusters was two (Figure 6B).

The sample comprised 93 patients in cluster 1 (C1) versus 59 patients in cluster 2 (C2). As demonstrated by the PCA scatter plot, there was a clear distinction in gene expression between the two subtypes, with a high degree of similarity observed within the subtypes (Figure 6C). This novel classification differed significantly from classical activity and severity staging (Figure 6D). In order to assess the robustness of the two molecular subtypes, a bootstrap resampling technique was employed, with 100 iterations being performed. The clustering solution exhibited excellent stability, with a median ARI of 0.9208 and a mean ARI of 0.9129 (95% CI: 0.753-1.0), confirming high reproducibility and robustness of the classification (Figure 6E). It was hypothesised that the addition would be advantageous to the prevailing grading and staging system of TED, with the potential to refine therapeutic recommendations.

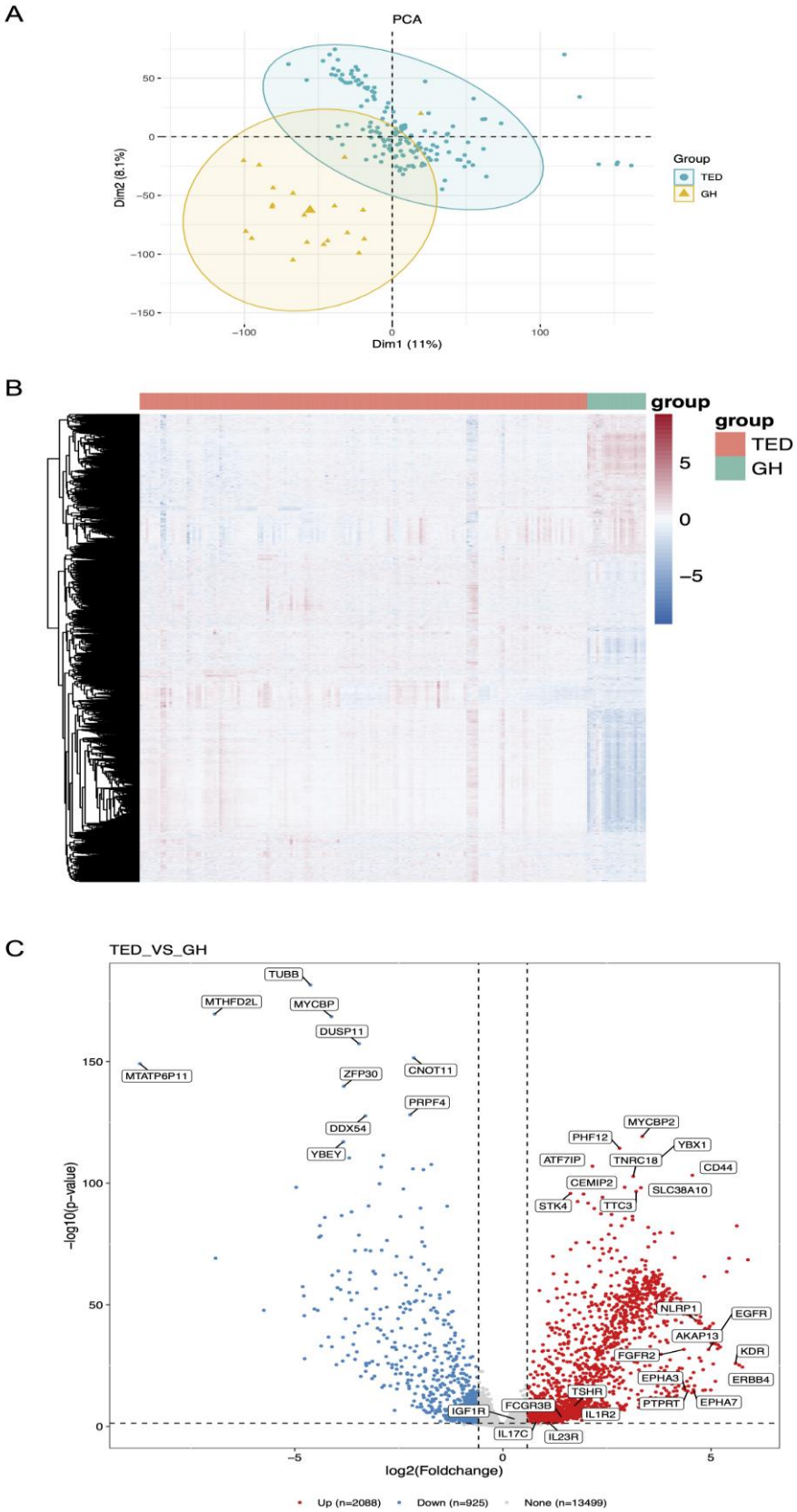

Figure 5. Overall Disparities in Gene Expression Profiles and the Identification of DEGs in TED Patients Compared to GH Patients

(A) PCA showed high similarity in the same group and little overlap between the two groups. (B) Heatmap displayed notable differences in transcriptome expression profiles. (C) Volcano plot illustrated DEGs with 2088 upregulated genes and 925 downregulated genes.

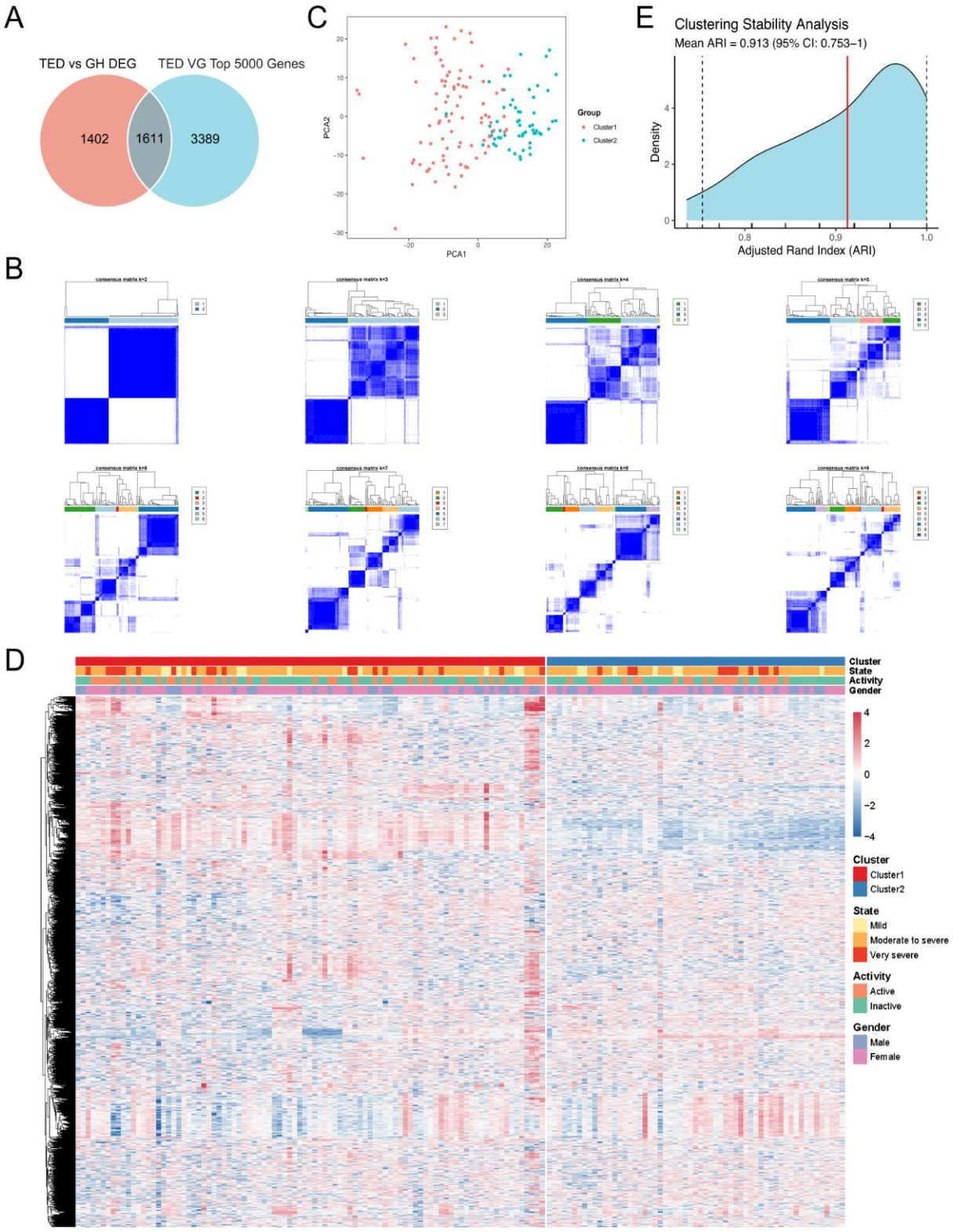

Figure 6. Unsupervised Clustering Divided TED Patients into Two Subtypes

(A) Venn plot showed the intersection of gene sets for unsupervised clustering. **(B)** The optic number of clusters was two. **(C)** PCA presented large difference between the two subtypes and high similarity within the subtypes. **(D)** Heatmap described distinct distribution of TED patients from classical assessment of severity and activity. C1 n=93; C2 n=59. **(E)** The stability of the clustering solution was evaluated using bootstrap resampling (mean ARI = 0.913, 95% CI: 0.753-1.0).

3.3 Two Subtypes of TED Patients Had Different Clinical Manifestations

No significant difference was tested in sex, age,

disease duration, activity and severity between the two subtypes (Table 5). C2 demonstrated a higher occurrence rate of spontaneous retrobulbar pain (p-value < 0.001) and attempted upward or downward gaze pain (p-value < 0.001). Furthermore, the subjects exhibited an increased propensity for lacrimation, as evidenced by a decline in basal tear production (p-value = 0.023) and an escalation in reflex epiphora (p-value = 0.017).

As anticipated, the thyroid function exhibited marked variations between the two clusters, attributable to elevated levels of free thyroxine (fT4) in C2 (Table 6). Importantly, other clinical indicators such as thyroid function parameters like thyroid stimulating hormone (TSH), free triiodothyronine (fT3) and TRAb, ophthalmology evaluations, and symptom prevalence were not significantly different between the two clusters (all P > 0.05; Table 7), indicating that the consensus clustering approach revealed intrinsic molecular heterogeneity beyond symptoms and highlighted the added value of transcriptomic stratification. Whilst the functional status of the thyroid has not been considered in the grading of TED according to guidelines, in clinical practice, the normalization of thyroid function is considered to be an essential endocrinological tactic in the treatment of the condition. Consequently, thyroid function may be subtly implicated in the refined diagnosis of TED, and may influence the selection of medication.

The two TED clusters exhibited no significant differences in activity or severity, but showed significant variations in risk factors, ocular pain, and reflex epiphora, suggesting that this classification approach offers a novel and important perspective.

Table 5. Basic Information of the New Subtypes of TED Patients

	C1	C2	p-value
No. of participants included	93	59	
Sex, M/F	30/63	22/37	0.524
Age, mean±SD (range), y	42.01±12.69 (18-65)	43.63±13.77 (18-74)	0.460
Duration of TED, median (IQR), m	14 (6-30)	12 (7-32)	0.970
Activity, active/inactive	38/55	22/37	0.661
Severity, mild/moderate-to-severe/sight-threatening severe	12/62/19	7/41/11	0.927

The statistical significance of age was assessed through the implementation of a two-sided t-test, given its conformance to a normal distribution and the presence of a chi-squared variance between the two clusters. The assessment of statistical significance for the duration of TED and severity was conducted through the utilisation of a two-sided rank sum test, because these variables were not normal distributed and severity had the ordinal nature. The evaluation of statistical significance for sex and activity was performed through the application of a chi-square test.

Table 6. Clinical Characteristics Significantly Different between the Two Subtypes

	C1	C2	p-value
No. of participants included	93	59	
Spontaneous retrobulbar pain, %	8.3	30.6	<0.001
Pain on attempted upward or downward gaze, %	2.4	22.4	<0.001
Reflex epiphora, %	51.6	71.2	0.017
Schirmer, 0~5 cm/5~10 cm/>10 cm	15/7/27	11/7/5	0.023
fT4, median (IQR), ng/dL	6.47 (0.93-15.22)	10.36 (0.86-16.24)	0.021
Smoking history, %	11.5	25.0	0.038
Smoking index, median (IQR)	150 (22.75-600)	300 (125-350)	0.022

The statistical significance of Schirmer, fT4 and smoking index was assessed through the implementation of a two-sided rank sum test, because these variables did not conform to a normal distribution. In order to assess statistical significance for spontaneous retrobulbar pain, pain on attempted upward or downward gaze, reflex epiphora and smoking history, a chi-square test was utilised.

Table 7. Insignificant Differences between the Two Clusters.

	C1	C2	p-value
No. of participants included	93	59	
Thyroid function			
TSH, median (IQR), μIU/mL	1.34 (0.02-2.88)	1.34 (0.01-3.90)	0.843
fT3, median (IQR), pg/mL	3.88 (3.30-4.77)	4.48 (3.21-5.86)	0.430
TRAb, median (IQR), IU/L	2.87 (1.43-21.79)	4.37 (1.95-12.70)	0.372
Ophthalmology evaluation			
BCVA, median (IQR)			
OD	1.0 (0.8-1.0)	1.00(0.85-1.0)	0.204
OS	1.0 (0.8-1.0)	1.0 (0.85-1.0)	0.490
IOP, median (IQR), mmHg			
OD	17.60 (16-20)	17.50 (15-18.25)	0.881
OS	18.00 (16-20.30)	18.00 (16-21)	0.865
Exophthalmos, mean±SD, mm			
OD	19.65±2.81	19.92±2.70	0.114
OS	19.67±3.07	19.97±2.96	0.068
MRD1, mean±SD, mm			
OD	4.03±1.64	4.67±1.75	0.681
OS	4.34±1.56	3.94±2.04	0.835
MRD2, mean±SD, mm			
OD	5.26±1.29	5.39±1.38	0.573
OS	5.57±1.34	6.03±1.48	0.244
BUT, median (IQR), s	7.65 (4.01-10.90)	10.33 (5.21-17.84)	0.100
Symptoms			
Blurred vision, Yes/No	23/62	17/35	0.482
Diplopia, Yes/No	39/45	30/23	0.246
Eyelid retraction, Yes/No	45/39	33/20	0.317
Photophobia, Yes/No	49/35	36/16	0.202
Dry eye, Yes/No	29/55	22/30	0.362

The independent samples t-test (two-tailed) tested differences between clusters for exophthalmos, MRD1, and MRD2. The Mann-Whitney U test (two-tailed) calculated differences between clusters for TSH, fT3, TRAb, BCVA, IOP, and BUT. Pearson's chi-square test (two-tailed) was employed for categorical variables.

3.4 The Two TED Subtypes Exhibited Distinct Patterns of Immune Infiltration

Immune infiltration analysis demonstrated that for both clusters, the quantities of myeloid-derived suppressor cells (MDSC), monocytes and immature B cells were higher than that of Th17 cells, eosinophils and Th2 cells in general (Figure 7A). It has been established that MDSC act as precursors to dendritic cells, macrophages and granulocytes[34]. Furthermore, MDSC have been shown to be capable of inhibiting immune responses. In pathological circumstances, the maturation of myeloid precursor cells is blocked, resulting in the production of immunosuppressive MDSC[35]. In condition of autoimmune diseases, MDSC act as considerable perplexity, characterised by a reactive increase and immune responses inhibition[36,37]. In this instance, the number of MDSC was found to be elevated in TED.

Subsequently, an immune cell comparison was conducted between the two clusters. A marked increase in the number of activated $CD4^+$ T cells, central memory $CD8^+$ T cells, follicular T helper cells, memory B cells and natural killer (NK) cells, particularly $CD56^{dim}$ NK cells, was observed in C1 compared to C2. Conversely, Th1 cells, Th17 cells and eosinophils exhibited a significant increase in C2 (Figure 7B). It is imperative to elucidate that, in an ideal scenario, PBMC isolated *via* Ficoll centrifugation should be devoid of eosinophils. Consequently, the eosinophil-related data presented herein were derived from computational analysis, which estimates cell-type-specific signatures as opposed to directly quantifying actual cell populations.

In comparison with C2, C1 demonstrated increased levels of adaptive immune cells, suggesting robust and well-established adaptive immune responses. This finding demonstrates that C1 displays more vigorous humoral immune activation and cytotoxic activity, while C2 exhibits a potent and destructive inflammatory response.

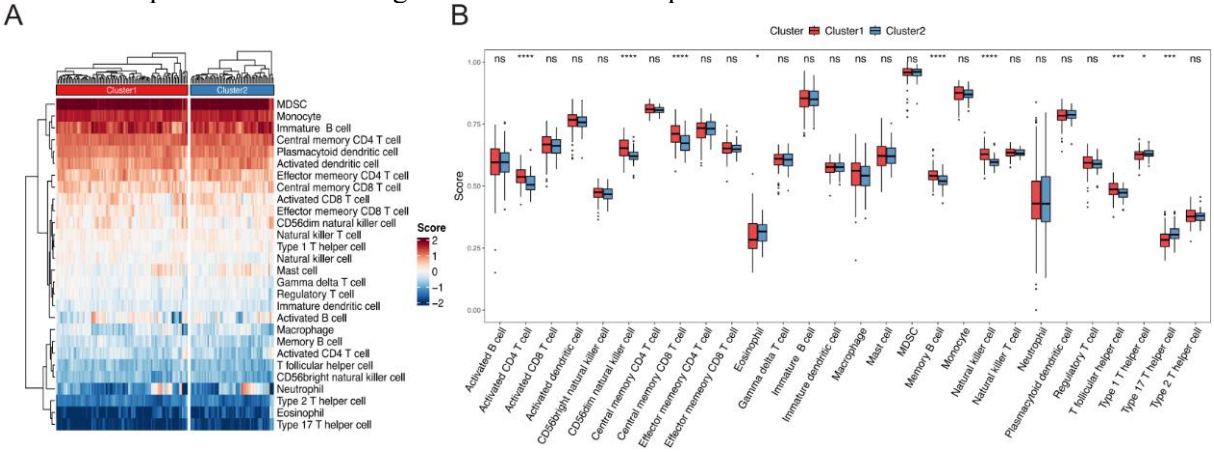

Figure 7. Immune Infiltration Analysis Based on ssGSEA among Two Clusters of TED Patients

(A) Heatmap showed the fraction of immune cells across C1 and C2 according to immune infiltration scores. **(B)** Boxplot exhibited six immune cells upregulated in C1 and three immune cells upregulated in C2. * means p-value < 0.05, ** means p-value < 0.01, *** means p-value < 0.001, and **** means p-value < 0.0001.

3.5 Representative Hub Genes were Defined in Each TED Subtypes

WGCNA was employed on the two clusters, and soft threshold was 8 (Figure 8A-B). Fourteen distinct gene modules with analogous co-expression patterns were detected (Figure 8C-D). The greenyellow module and the green module were found to be most closely associated with C1 and C2, respectively (Figure 8E).

GO analysis of the greenyellow module revealed that C1 exhibited powerful adaptive immune responses, particularly B cell activation and antibody responses. PI3KB signal transduction and MAPK cascade were identified as key intracellular signalling routes supporting cell survival and proliferation. In order to accommodate such rapid proliferation, it was hypothesised that DNA repair and autophagy mechanisms would be concomitantly activated. Furthermore, the observed enrichment of wound healing and the organisation of actin filaments indicated the occurrence of tissue remodelling and repair, which may be associated with pathogenic mechanisms following immune cell homing (Figure 8F). KEGG analysis similarly indicated that C1 presented as intense adaptive immunity, pro-survival and anti-apoptotic signalling, metabolic reprogramming, and tissue remodelling potentially associated with lesion pathogenesis (Figure 8G). Conversely, C2 exhibited significant activation centred on the RNA splicing pathway, suggesting that this cluster may be experiencing an acute and destructive immune activation state (Figure 8F-G).

In order to enhance the clarity and generalisability of the classification scheme, LASSO regression was employed on genes from the greenyellow and green modules, leading to the identification of nine hub genes (see Figure 9A-B). Six of these were found to be C1-specific: discoidin domain receptor tyrosine kinase 2 (DDR2), LDL receptor related protein 1B (LRP1B), NTRK2, partner and localizer of BRCA2 (PALB2), protein tyrosine phosphatase receptor type D (PTPRD) and solute carrier family 25 member 6 (SLC25A6). In addition, three were found to be C2-specific: MON2 homolog regulator of endosome-to-Golgi trafficking (MON2), small nucleolar RNA H/ACA Box 74B (SNORA74B) and syntaxin 16 (STX16).

In summary, the C1 subtype is characterised by sustained adaptive immune responses, coupled with cellular proliferation and metabolism. This has led to its designation as the "adaptive and proliferative" subtype. Conversely, C2 displays features of acute and destructive inflammatory responses, termed the "inflammatory and destructive" subtype. The nine hub genes have been identified as being highly correlated and convergent with the typing phenotype. These genes can be leveraged to simplify classification

and facilitate precise diagnosis.

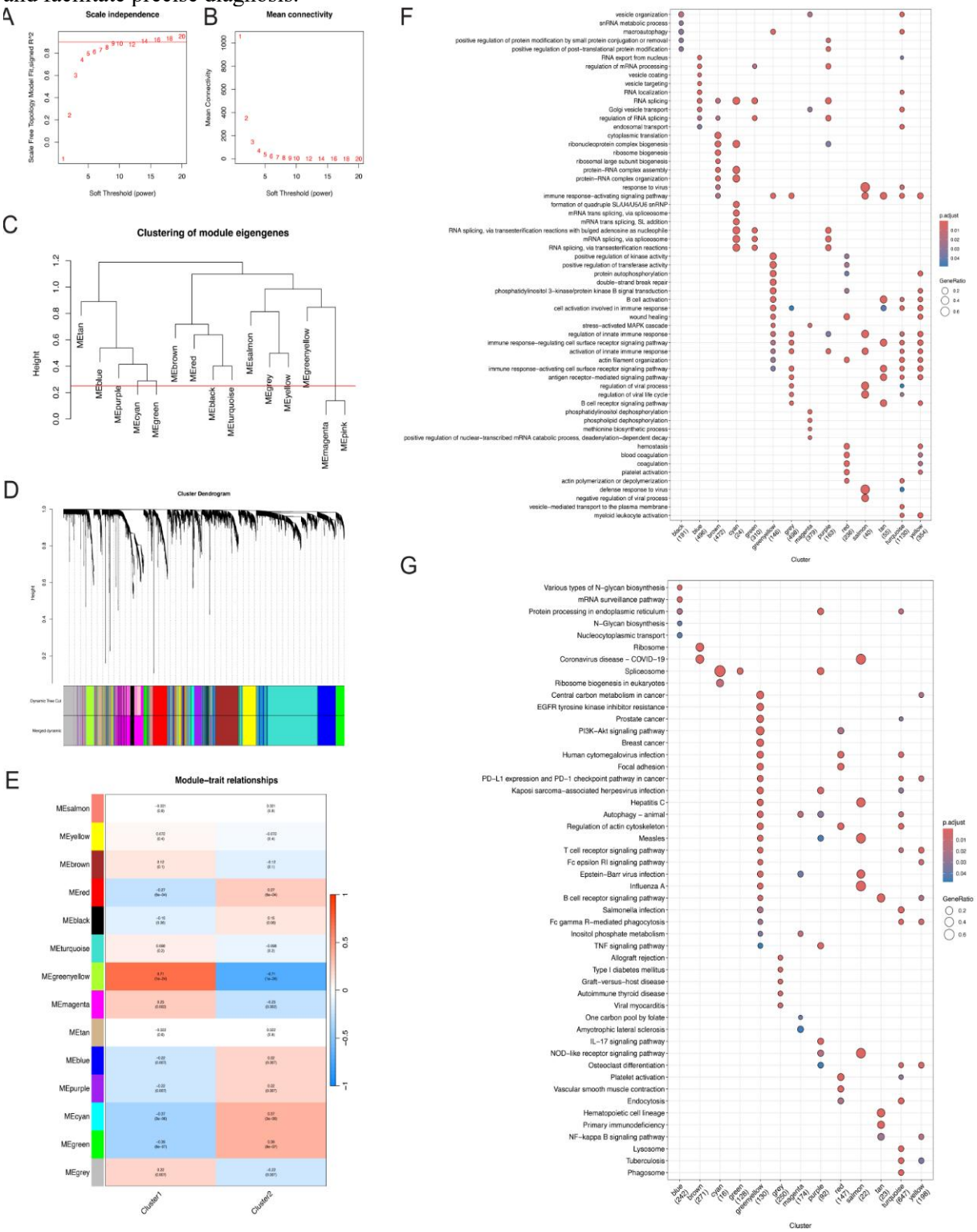

Figure 8. WGCNA across the Two Clusters of TED Patients

(A-B) Optimal soft threshold was chosen as 8. **(C)** Genes categorization by TOM dissimilarity measure based on the average linkage hierarchical clustering (minModuleSize = 30). **(D)** Gene hierarchy clustering dendrogram showed fourteen distinct gene modules. **(E)** Heatmap reflected the greenyellow module and green module were most closely related to C1 and C2 respectively. **(F)** Top 10 pathways in every module by GO analysis. **(G)** Top 10 pathways in every module by KEGG analysis.

Abbr: TOM: topological overlap matrix.

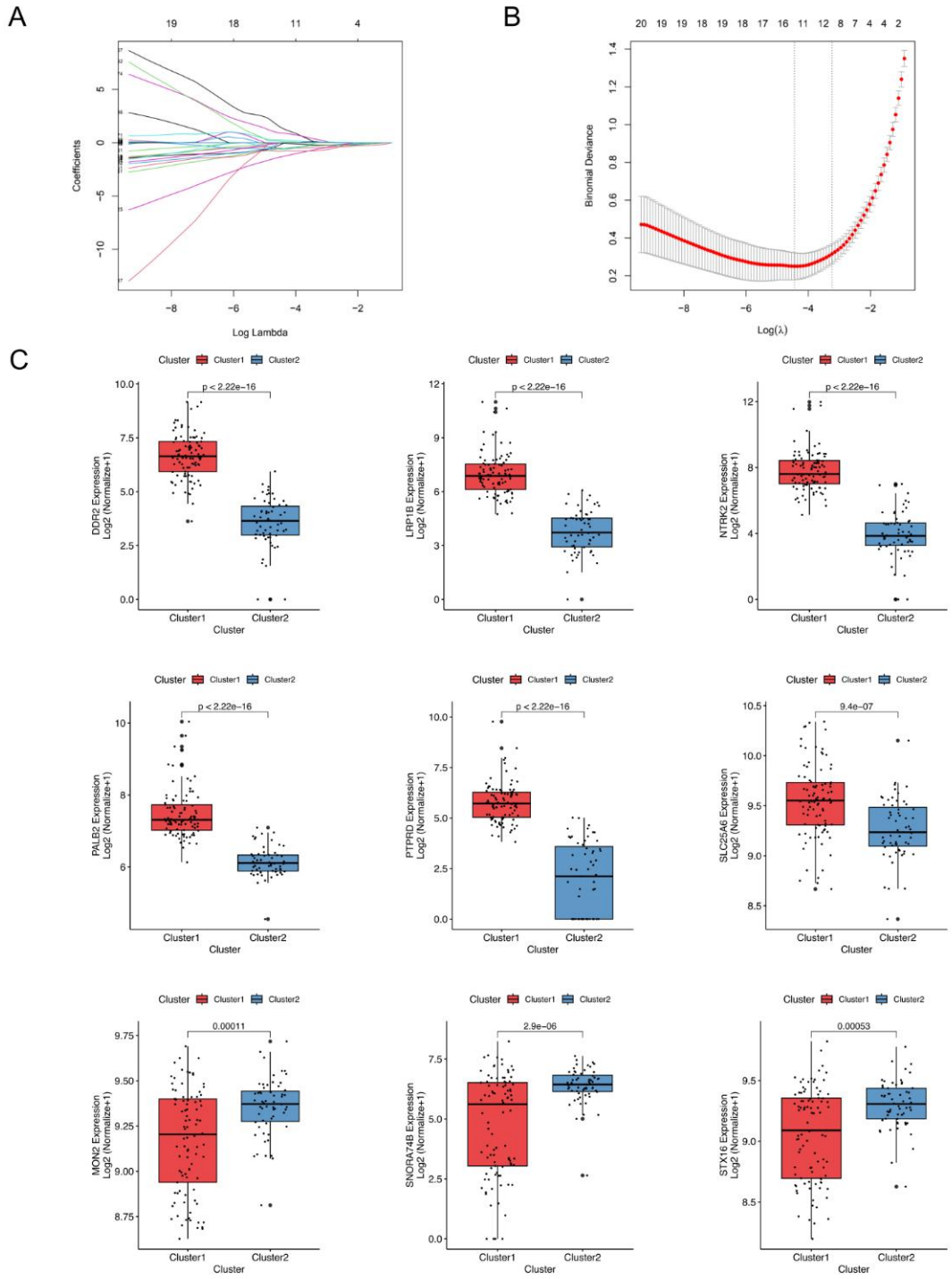

Figure 9. LASSO Regression and Hub Genes Representing the Two Clusters

(A) LASSO coefficient profiles: candidate gene expression. **(B)** Cross-validation of LASSO model. **(C)** LASSO linear regression of genes from green and greenyellow modules with 9 hub genes.

3.6 Patients of the Two Subtypes Had Different Sensitivity to Drug Targets

The analysis of drug sensitivity, based on transcriptomic profiles, predicted distinct therapeutic vulnerabilities for the two subtypes. For subtype C1, several compounds were identified as potentially effective, including the sulfonylurea gliquidone, the Janus kinase inhibitor AT-9283, the IκB kinase inhibitor BX-795, and multiple growth factor receptor inhibitors (axitinib, orantinib, MAZ-51) (Figure 10A). The predicted mechanisms of action associated with these compounds included tubulin inhibition, glutamate receptor antagonism, glycogen synthase kinase inhibition, platelet-derived growth factor receptor inhibition, and protein kinase C (PKC) activation.

In contrast, subtype C2 exhibited predicted sensitivity to a different set of compounds, including the cannabinoid receptor agonist oleylethanolamide, the glucocorticoid receptor agonist prednisone, the DNA-binding agent bisbenzimide, and the anti-inflammatory agent celastrol (Figure 10B). The mechanisms associated with these agents encompassed broad-spectrum anti-inflammatory and immunosuppressive effects, as well as direct interference with DNA structure and function.

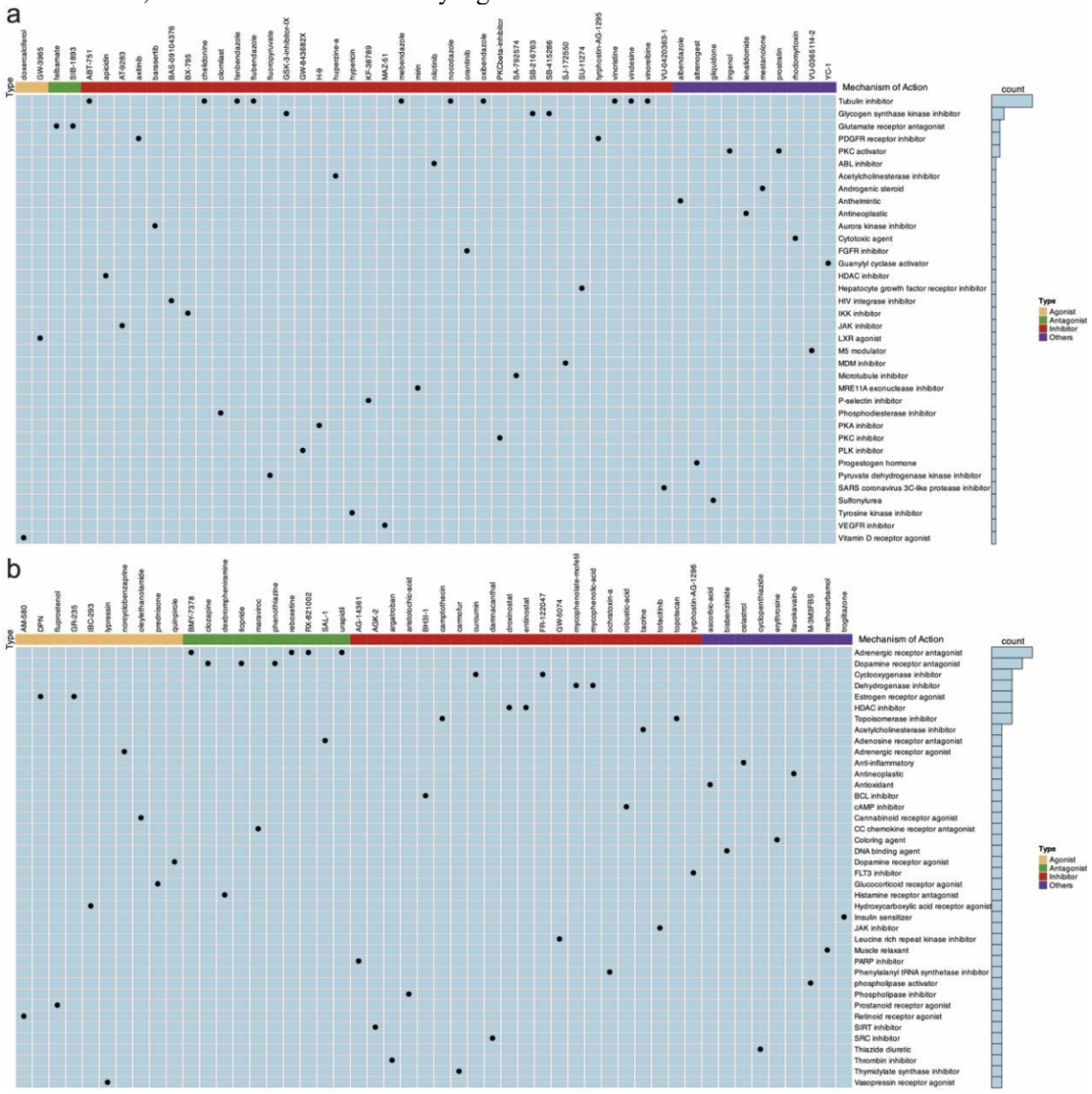

Figure 10. Drug Sensitivity Analysis for Each Cluster of TED Based on CMap

(A) Potential mechanisms and corresponding drugs for C1. **(B)** Potential mechanisms and corresponding drugs for C2.

4. Discussion

TED is an autoimmune disorder with heterogeneous clinical presentation, currently managed according to activity and severity. Patients with non-surgical TED face a range of therapeutic interventions with limited response rates, underscoring the urgent need for more precise classifications. Consequently, the present study established the first large-scale cohort for TED and controls, and performed the first genuine molecular classification of TED. This classification system utilises key hub genes to predict drug sensitivity and provides insights into the unique pathological characteristics of each subtype.

The present study has revealed that TED is characterised by elevated autoantigens, immune

overactivation, cell proliferation, and metabolic dysregulation. Intriguingly, receptor tyrosine kinases (RTKs) such as EGFR and NTRK have got attention in TED pathogenesis. EGFR was observed to promote focal adhesion through the PI3K/Akt pathway, thereby the recruitment of circulating T cells was fostered to the orbit in TED[38]. The activation of EGFR promoter has been observed to be induced by the highly expressed SRY-Box transcription factor 9 (SOX9) on fibroblasts in the orbit, resulting in the subsequent MAPK pathway-mediated fibrosis[39]. The present findings are in alignment with these observations, thus suggesting that EGFR contributes to the pathogenesis of TED by means of enhancing T cell homing and fibrosis. Despite the paucity of research conducted on NTRK in the context of TED, NTRK fusions have been observed to induce constitutive proliferation and inhibit apoptosis[40]. In view of the primary function of NTRK[41,42], it is hypothesised that its elevated expression in TED may promote immune cell proliferation and energy metabolism *via* the MAPK and PI3K/Akt pathways. In addition, the possibility of outcomes like optic neuropathy, cerebral alterations, and neuropsychiatric symptoms[43-45] raises the concern about the pivotal role of NTRK in neuroplasticity and eye-brain communication.

Another significant contribution of this study is the classification of TED patients into two distinct clusters. C1 is indicative of the "adaptive and proliferative" subtype, whereas C2 denotes the "inflammatory and destructive" subtype. Decoupled from activity and severity, this taxonomy is more sensitive and forward-looking. Indeed, molecular classification is a highly active field of research in oncology[46,47], as well as in the realm of inflammatory and autoimmune diseases, including knee osteoarthritis, Sjögren's syndrome, and inflammatory palmoplantar keratoderma[48-50]. This study represents the initial phase of the TED research project, and the observed concordance among clinical manifestations and gene signatures highlights the translational potential of the research.

It is noteworthy that the two subtypes exhibited a discrepancy in fT4 levels despite the clinical homogeneity observed in other thyroid parameters. This biochemical discrepancy suggests that molecular stratification may capture subtle endocrinological variations that are overlooked by conventional clinical assessments. Conventionally, clinical attention in TED has been predominantly focused on TRAb as the key serological marker for both diagnosis and disease monitoring. However, the present findings suggest that fT4 may also have previously underappreciated significance. This suggests the intriguing possibility that fT4, in addition to its role as a hormone, may be a surrogate indicator for underlying immune-metabolic status in TED. The necessity for prospective studies is evident in order to determine whether this fT4 elevation correlates with disease progression or response to therapy. Furthermore, it is important to ascertain whether integrating fT4 with existing biomarkers like TRAb could refine patient stratification and personalised management.

The implementation of molecular classification is hindered by two primary factors: the significant financial investment required and the lack of standardisation in data pipelines. The utilisation of screened hub genes has been posited as a potential solution to these challenges. DDR2, also known as neurotrophic tyrosine kinase receptor-related 3 (NTRKR3), has been shown to interact with collagen, thereby regulating procedures including cell growth, differentiation, as well as metabolism. Inhibition of DDR2 has been demonstrated to impede myofibroblast activation and neovascularization in pulmonary fibrosis[51]. Despite the absence of any mention of DDR2 in TED, there is a clear correlation between its profibrotic and proangiogenic functions in fibrotic diseases and the effects observed. The present study demonstrated that LRP1B knockdown decreased enzymes associated with lipid synthesis, whilst concurrently increasing the expression of enzymes related to β-oxidation and the AMPK signalling pathway[52]. As evidenced by the finding that AMPK blockers enhance lipid accumulation in TED, which is characterised by adiposis of orbital fibroblasts[53], LRP1B may help generate adipose tissue in TED. The PTPRD/CXCL8 axis has been pivotal in the amplification of angiogenesis and metastasis in gastric cancer[54]. As demonstrated in the extant literature, there is a demonstrable uprise in CXCR3 in the orbital connective tissue and conjunctival epithelium during the chronic phase of TED[55-57]. PTPRD is a potential novel modulator of inflammation and vascularization in TED. The mechanisms underlying hub genes

remain to be elucidated; however, they have the potential to serve as biomarkers in the preliminary phase.

In addition to the utilisation of efficient hub genes, this classification provides practical guidance for the selection of TED drugs. At present, the criteria for determining suitable patients for targeted therapies in TED are fragmented. Teprotumumab is recommended for cases of active moderate-to-severe TED that suffer from proptosis and double vision. Rituximab is preferred for intractable TED, with beneficial effects in terms of relapse prevention, especially when administered within 9 months of the initial diagnosis. Tocilizumab has been demonstrated to be an effective therapeutic option for patients who did not get expected outcomes from glucocorticoid therapy and who are suffering from moderate-to-severe TED[6]. The drug sensitivity profiles predicted in this study offer a molecular rationale that may complement the existing clinical criteria. For instance, the C1 sub-type exhibited predicted sensitivity to multiple kinase inhibitors, aligning mechanistically with the mechanism of Teprotumumab and suggesting a potential molecular basis for patient selection for such targeted therapies. In contrast, subtype C2 exhibited predicted sensitivity to glucocorticoids, consistent with its role as first-line immunotherapy and providing a possible explanation for the variable clinical responses observed among TED patients. The present system does not seek to replace the classical grading system (severity and activity), but rather to provide a refined subclassification for patients with refractory disease. This molecular typing is of particular value as a reference for active moderate to severe TED, constituting the largest proportion of cases and have the most targeted treatment options.

The decision to utilise peripheral blood as opposed to orbital tissue as the sample source is predicated on the fact that it can be obtained prior to the commencement of treatment, thereby providing a reflection of the systemic status. The present study is not without its limitations. Firstly, given the relatively limited sample and the absence of an external validation cohort, the broader applicability of these findings remains to be established. Secondly, the clustering model is deficient in long-term follow-up to observe the real responses of different therapies. Thirdly, the hub genes have not been validated with regard to their role in tissue-specific pathology. In the subsequent phases of this research series, the objective is to recruit multi-center cohorts for the long-term, systematic validation of three dimensions (model, simplified diagnostic frameworks, and biological mechanisms), building upon the foundational findings of the present study.

5. Conclusions

In conclusion, transcriptomic profiling delineated TED by elevated autoantigens, immune activation, cell proliferation, and metabolic dysregulation. Following a diagnosis, TED can be categorised into two distinct subtypes based on gene signatures, which significantly differ in clinical presentations such as ocular pain and reflex epiphora. The two subtypes manifest distinct proliferation patterns of immune cell subpopulations and exhibit divergent pathophysiological characteristics. This binary molecular classification, navigated by hub genes, has the capacity to indicate drug preferences with regard to activity and severity. The consequence of this is that it can promote personalised therapy in TED.

Acknowledgments

This study was supported by the National Natural Science Foundation of China (82301258), Chang Jiang Scholars Program (T2022065), the Sample Biobank Project of Shanghai Ninth People’s Hospital (YBKB202211).

References

[1] TAYLOR P N, ZHANG L, LEE R W J, et al. New insights into the pathogenesis and nonsurgical management of Graves orbitopathy. Nat Rev Endocrinol, 2020, 16(2): 104-16.

[2] BAHN R S. Graves' ophthalmopathy. N Engl J Med, 2010, 362(8): 726-38.

[3] CUI X, WANG F, LIU C. A review of TSHR- and IGF-1R-related pathogenesis and treatment of Graves' orbitopathy. Front Immunol, 2023, 14: 1062045.

[4] BARTALENA L, GALLO D, TANDA M L, et al. Thyroid Eye Disease: Epidemiology, Natural History, and Risk Factors. Ophthalmic Plast Reconstr Surg, 2023, 39(6s): S2-s8.

[5] SHARMA A, STAN M N, ROOTMAN D B. Measuring Health-Related Quality of

Life in Thyroid Eye Disease. J Clin Endocrinol Metab, 2022, 107(Suppl_1): S27-s35.
[6] BURCH H B, PERROS P, BEDNARCZUK T, et al. Management of Thyroid Eye Disease: A Consensus Statement by the American Thyroid Association and the European Thyroid Association. Thyroid, 2022, 32(12): 1439-70.
[7] LäNGERICHT J, KRäMER I, KAHALY G J. Glucocorticoids in Graves' orbitopathy: mechanisms of action and clinical application. Ther Adv Endocrinol Metab, 2020, 11: 2042018820958335.
[8] BARTALENA L, KRASSAS G E, WIERSINGA W, et al. Efficacy and safety of three different cumulative doses of intravenous methylprednisolone for moderate to severe and active Graves' orbitopathy. J Clin Endocrinol Metab, 2012, 97(12): 4454-63.
[9] DOUGLAS R S, KAHALY G J, PATEL A, et al. Teprotumumab for the Treatment of Active Thyroid Eye Disease. N Engl J Med, 2020, 382(4): 341-52.
[10] KAHALY G J, DOUGLAS R S, HOLT R J, et al. Teprotumumab for patients with active thyroid eye disease: a pooled data analysis, subgroup analyses, and off-treatment follow-up results from two randomised, double-masked, placebo-controlled, multicentre trials. Lancet Diabetes Endocrinol, 2021, 9(6): 360-72.
[11]DOUGLAS R S, KAHALY G J, UGRADAR S, et al. Teprotumumab Efficacy, Safety, and Durability in Longer-Duration Thyroid Eye Disease and Re-treatment: OPTIC-X Study. Ophthalmology, 2022, 129(4): 438-49.
[12]UGRADAR S, MALKHASYAN E, DOUGLAS R S. Teprotumumab for the Treatment of Thyroid Eye Disease. Endocr Rev, 2024, 45(6): 843-57.
[13]QIAN W, ZHU T, LIU J, et al. Integrative transcriptomic profiling and machine learning reveal hypoxia-associated molecular signatures for precision diagnosis in thyroid eye disease. Hum Genomics, 2025, 19(1): 140.
[14]LIU J, QIAN W, YANG L, et al. A machine learning-based model for the prediction of thyroid eye disease with oxidative stress-related biomarkers. Exp Eye Res, 2026, 264: 110835.
[15]RUBIN P A, WATKINS L M, RUMELT S, et al. Orbital computed tomographic characteristics of globe subluxation in thyroid orbitopathy. Ophthalmology, 1998, 105(11): 2061-4.
[16]KURIYAN A E, WOELLER C F, O'LOUGHLIN C W, et al. Orbital fibroblasts from thyroid eye disease patients differ in proliferative and adipogenic responses depending on disease subtype. Invest Ophthalmol Vis Sci, 2013, 54(12): 7370-7.
[17]SY A, SILKISS R Z. Serum total IgG and IgG4 levels in thyroid eye disease. Int Med Case Rep J, 2016, 9: 325-8.
[18]MIZOKAMI T, SALVI M, WALL J R. Eye muscle antibodies in Graves' ophthalmopathy: pathogenic or secondary epiphenomenon?. J Endocrinol Invest, 2004, 27(3): 221-9.
[19]ALVES JUNIOR J M, BERNARDO W, VILLAGELIN D. Effectiveness of Different Treatment Modalities in Initial and Chronic Phases of Thyroid Eye Disease: A Systematic Review With Meta-analysis. J Clin Endocrinol Metab, 2024, 109(11): 2997-3009.
[20]Gene Expression Omnibus. GSE280114.
[21]Gene Expression Omnibus. GSE285190.
[22]LOVE M I, HUBER W, ANDERS S. Moderated estimation of fold change and dispersion for RNA-seq data with DESeq2. Genome Biol, 2014, 15(12): 550.
[23]The Gene Ontology Resource: 20 years and still GOing strong. Nucleic Acids Res, 2019, 47(D1): D330-d8.
[24]KANEHISA M, GOTO S. KEGG: kyoto encyclopedia of genes and genomes. Nucleic Acids Res, 2000, 28(1): 27-30.
[25]YU G, WANG L G, HAN Y, et al. clusterProfiler: an R package for comparing biological themes among gene clusters. Omics, 2012, 16(5): 284-7.
[26]LIBERZON A, BIRGER C, THORVALDSDóTTIR H, et al. The Molecular Signatures Database (MSigDB) hallmark gene set collection. Cell Syst, 2015, 1(6): 417-25.
[27]SUBRAMANIAN A, TAMAYO P, MOOTHA V K, et al. Gene set enrichment analysis: a knowledge-based approach for interpreting genome-wide

expression profiles. Proc Natl Acad Sci U S A, 2005, 102(43): 15545-50.
[28]WILKERSON M D, HAYES D N. ConsensusClusterPlus: a class discovery tool with confidence assessments and item tracking. Bioinformatics, 2010, 26(12): 1572-3.
[29]ZHENG H, LIU H, LI H, et al. Characterization of stem cell landscape and identification of stemness-relevant prognostic gene signature to aid immunotherapy in colorectal cancer. Stem Cell Res Ther, 2022, 13(1): 244.
[30]CHAROENTONG P, FINOTELLO F, ANGELOVA M, et al. Pan-cancer Immunogenomic Analyses Reveal Genotype-Immunophenotype Relationships and Predictors of Response to Checkpoint Blockade. Cell Rep, 2017, 18(1): 248-62.
[31]LANGFELDER P, HORVATH S. WGCNA: an R package for weighted correlation network analysis. BMC Bioinformatics, 2008, 9: 559.
[32]LAMB J, CRAWFORD E D, PECK D, et al. The Connectivity Map: using gene-expression signatures to connect small molecules, genes, and disease. Science, 2006, 313(5795): 1929-35.
[33]GU Z. Complex heatmap visualization. Imeta, 2022, 1(3): e43.
[34]HEGDE S, LEADER A M, MERAD M. MDSC: Markers, development, states, and unaddressed complexity. Immunity, 2021, 54(5): 875-84.
[35]VEGLIA F, PEREGO M, GABRILOVICH D. Myeloid-derived suppressor cells coming of age. Nat Immunol, 2018, 19(2): 108-19.
[36]IWATA Y, FURUICHI K, KITAGAWA K, et al. Involvement of CD11b+ GR-1 low cells in autoimmune disorder in MRL-Fas lpr mouse. Clin Exp Nephrol, 2010, 14(5): 411-7.
[37]PARK M J, LEE S H, KIM E K, et al. Myeloid-Derived Suppressor Cells Induce the Expansion of Regulatory B Cells and Ameliorate Autoimmunity in the Sanroque Mouse Model of Systemic Lupus Erythematosus. Arthritis Rheumatol, 2016, 68(11): 2717-27.
[38]WANG N, HOU S Y, QI X, et al. LncRNA LPAL2/miR-1287-5p/EGFR Axis Modulates TED-Derived Orbital Fibroblast Activation Through Cell Adhesion Factors. J Clin Endocrinol Metab, 2021, 106(8): e2866-e86.
[39]ZHOU M, LIN B, WU P, et al. SOX9 Induces Orbital Fibroblast Activation in Thyroid Eye Disease Via MAPK/ERK1/2 Pathway. Invest Ophthalmol Vis Sci, 2024, 65(2): 25.
[40]SOLOMON J P, BENAYED R, HECHTMAN J F, et al. Identifying patients with NTRK fusion cancer. Ann Oncol, 2019, 30(Suppl_8): viii16-viii22.
[41]KHOTSKAYA Y B, HOLLA V R, FARAGO A F, et al. Targeting TRK family proteins in cancer. Pharmacol Ther, 2017, 173: 58-66.
[42]JIN W, YUN C, HOBBIE A, et al. Cellular transformation and activation of the phosphoinositide-3-kinase-Akt cascade by the ETV6-NTRK3 chimeric tyrosine kinase requires c-Src. Cancer Res, 2007, 67(7): 3192-200.
[43]JOHNSON B T, JAMEYFIELD E, AAKALU V K. Optic neuropathy and diplopia from thyroid eye disease: update on pathophysiology and treatment. Curr Opin Neurol, 2021, 34(1): 116-21.
[44]ZHANG H, LIU Y, ZHANG Z, et al. Neuroimaging in thyroid eye disease: A systematic review. Autoimmun Rev, 2024, 23(12): 103667.
[45]BRUSCOLINI A, SACCHETTI M, LA CAVA M, et al. Quality of life and neuropsychiatric disorders in patients with Graves' Orbitopathy: Current concepts. Autoimmun Rev, 2018, 17(7): 639-43.
[46]LIU Z, ZHAO Y, KONG P, et al. Integrated multi-omics profiling yields a clinically relevant molecular classification for esophageal squamous cell carcinoma. Cancer Cell, 2023, 41(1): 181-95.e9.
[47]PAJTLER K W, WITT H, SILL M, et al. Molecular Classification of Ependymal Tumors across All CNS Compartments, Histopathological Grades, and Age Groups. Cancer Cell, 2015, 27(5): 728-43.
[48]LV Z, YANG Y X, LI J, et al. Molecular Classification of Knee Osteoarthritis. Front Cell Dev Biol, 2021, 9: 725568.
[49]SORET P, LE DANTEC C, DESVAUX E, et al. A new molecular classification to drive precision treatment strategies in

primary Sjögren's syndrome. Nat Commun, 2021, 12(1): 3523.
[50]VAN STRAALEN K R, KIRMA J, YEE C M, et al. Disease heterogeneity and molecular classification of inflammatory palmoplantar diseases. J Allergy Clin Immunol, 2024, 154(5): 1204-15.e9.
[51]ZHAO H, BIAN H, BU X, et al. Targeting of Discoidin Domain Receptor 2 (DDR2) Prevents Myofibroblast Activation and Neovessel Formation During Pulmonary Fibrosis. Mol Ther, 2016, 24(10): 1734-44.
[52]LI M, HU J, JIN R, et al. Effects of LRP1B Regulated by HSF1 on Lipid Metabolism in Hepatocellular Carcinoma. J Hepatocell Carcinoma, 2020, 7: 361-76.
[53]HAMMOND C L, ROZTOCIL E, GONZALEZ M O, et al. MicroRNA-130a Is Elevated in Thyroid Eye Disease and Increases Lipid Accumulation in Fibroblasts Through the Suppression of AMPK. Invest Ophthalmol Vis Sci, 2021, 62(1): 29.
[54]BAE W J, AHN J M, BYEON H E, et al. PTPRD-inactivation-induced CXCL8 promotes angiogenesis and metastasis in gastric cancer and is inhibited by metformin. J Exp Clin Cancer Res, 2019, 38(1): 484.
[55]FERRARI S M, RAGUSA F, PAPARO S R, et al. Differential modulation of CXCL8 versus CXCL10, by cytokines, PPAR-gamma, or PPAR-alpha agonists, in primary cells from Graves' disease and ophthalmopathy. Autoimmun Rev, 2019, 18(7): 673-8.
[56]LI Z, WANG M, TAN J, et al. Single-cell RNA sequencing depicts the local cell landscape in thyroid-associated ophthalmopathy. Cell Rep Med, 2022, 3(8): 100699.
[57]BRUSCOLINI A, SEGATTO M, MARENCO M, et al. Alteration of CXCL8 pathway in the ocular surface of patients with Graves' orbitopathy. Autoimmun Rev, 2020, 19(12): 102682.

